Oral Oncology 86 (2018) 206–215

Contents lists available at ScienceDirect

Oral Oncology

journal homepage: www.elsevier.com/locate/oraloncology

Label-free tissue proteomics can classify oral squamous cell carcinoma from healthy tissue in a stage-specific manner

Amy Dickinson[a,b,*,1], Mayank Saraswat[a,d,1], Antti Mäkitie[b,e], Robert Silén[a], Jaana Hagström[d,h], Caj Haglund[f,g], Sakari Joenväärä[a,d], Suvi Silén[b,c]

[a] Transplantation Laboratory, Haartman Institute, University of Helsinki, Haartmaninkatu 3, PO Box 21, 00014, Finland
[b] Department of Otorhinolaryngology – Head and Neck Surgery, University of Helsinki and Helsinki University Hospital, Helsinki, Finland
[c] Department of Biosciences and Nutrition, Karolinska Institutet, Stockholm, Sweden
[d] HUSLAB, Helsinki University Hospital, Helsinki 00290, Finland
[e] Division of Ear, Nose and Throat Diseases, Department of Clinical Sciences, Intervention and Technology, Karolinska Institutet and Karolinska University Hospital, Stockholm, Sweden
[f] Department of Surgery, University of Helsinki and Helsinki, University Hospital, Helsinki, Finland
[g] Research Programs Unit, Translational Cancer Biology, University of Helsinki, Helsinki, Finland
[h] Department of Pathology, University of Helsinki, Finland

ARTICLE INFO

Keywords:
Oral squamous cell carcinoma
Head and neck cancer
Tongue cancer
OPLS-DA
Tissue proteomics
CA1
S100A7
Neutrophil defensin 1
ANP32B
Immunohistochemistry

ABSTRACT

Objectives: No prognostic or predictive biomarkers for oral squamous cell carcinoma (OSCC) exist. We aimed to discover novel proteins, altered in OSCC, to be further investigated as potential biomarkers, and to improve understanding about pathways involved in OSCC.
Materials and Methods: Proteomic signatures of seven paired healthy and OSCC tissue samples were identified using ultra-definition quantitative mass spectrometry, then analysed and compared using Anova, principal component analysis, hierarchical clustering and OPLS-DA modelling. A selection of significant proteins that were also altered in the serum from a previous study (PMID: 28632724) were validated immunohistochemically on an independent cohort (n = 66) to confirm immunopositivity and location within tumour tissue. Ingenuity Pathways Analysis was employed to identify altered pathways.
Results: Of 829 proteins quantified, 257 were significant and 72 were able to classify healthy vs OSCC using OPLS-DA modelling. We identified 19 proteins not previously known to be upregulated in OSCC, including prosaposin and alpha-taxilin. KIAA1217 and NDRG1 were upregulated in stage IVa compared with stage I tumours. Altered pathways included calcium signalling, cellular movement, haematological system development and function, and immune cell trafficking, and involved NF-kB and MAPK networks.
Conclusions: We found a set of proteins reliably separating OSCC tumour from healthy tissue, and multiple proteins differing between stage I and stage IVa OSCC. These potential biomarkers can be studied and validated in larger cohorts.

Abbreviations: ALYREF, THO complex subunit 4; ANP32B, Acidic leucine-rich nuclear phosphoprotein 32 family member B; AUROC, area under the receiver operating characteristic curve; BCA, bicinchoninic acid; CA1, carbonic anhydrase 1; CAIX, carbonic anhydrase IX; CYFRA-1, name of a test for soluble cytokeratin fragments; DEFA1, neutrophil defensin 1; DNAJC8, DnaJ homolog subfamily C member 8; DSS, disease-specific survival; DTT, dithiothreitol; EDTA, ethane-1,2-diyldinitrilotetraacetic acid; FC, mean fold change; H&E, haematoxylin and eosin; HCA, Hierarchical clustering analysis; HNSCC, head and neck squamous cell carcinoma; IAA, iodoacetamide; IHC, immunohistochemistry; IPA, Ingenuity pathway analysis; IP3R, Inositol triphosphate receptor; KIAA1217, sickle tail protein homologue; KRT, keratin; MAPK, mitogen activated protein kinase; MS, mass spectrometry; NAP1L1, nucleosome assembly protein 1-like 1; NDRG1, protein NDRG1; NF-κB, nuclear Factor-κB; nUPLC-UDMSE, Nano Ultra Performance Liquid Chromatography Label Free Ultra-definition mass spectrometry; OPLS-DA, Orthogonal Projections to Latent Structures Discriminant Analysis; OSCC, Oral squamous cell carcinoma; PABPN1, Polyadenylate-binding protein 2; PCA, Principal component analysis; PMCA1, plasma membrane Ca2+ ATPase isoform 1; PPI, protein-protein interactions; PSAP, prosaposin; SCLC, small cell lung cancer; STMN1, stathmin 1; TMA, tissue microarray; TNM, tumour-node-metastasis; TPA, cytokeratin detection test

* Corresponding author at: Transplantation Laboratory, Haartman Institute, University of Helsinki, Haartmaninkatu 3, PO Box 21, 00014, Finland.
E-mail addresses: Amy.dickinson@helsinki.fi (A. Dickinson), sarawat.mk@gmail.com (M. Saraswat), antti.makitie@helsinki.fi (A. Mäkitie), robert.silen@iki.fi (R. Silén), jaana.hagstrom@hus.fi (J. Hagström), caj.haglund@helsinki.fi (C. Haglund), sakari.joenvaara@helsinki.fi (S. Joenväärä), suvi.silen@helsinki.fi (S. Silén).
[1] These authors contributed equally to this work.

https://doi.org/10.1016/j.oraloncology.2018.09.013
Received 6 June 2018; Received in revised form 21 August 2018; Accepted 13 September 2018
Available online 03 October 2018
1368-8375/

Introduction

Oral squamous cell carcinoma (OSCC) is the most common type of head and neck cancer globally with an annual incidence of around 275 000 [1]. It is more prevalent in men, and prevalence is increasing [2]. In particular, tongue cancer incidence has been rising in various parts of the world in recent years, and especially in patients under 45 [1,3]. Strong risk factors include alcohol and tobacco.

Western 5-year survival rates for oral cavity cancer are around 60% [3–5]. Five-year disease- specific survival (DSS) of OSCC of the mobile tongue decreases as the stage increases. In Finland, 5-year DSS is 87% for stage I carcinomas, but 51% for stage IV. Interestingly, recurrence occurred in 22–34% of patients, slightly varying by stage [6].

However, the TNM classification does not fully account for OSCC patients' outcomes [7]; tumours with the same TNM stage can exhibit different behaviours, treatment responses, and prognoses [8]. Different molecules and pathways have been linked with OSCC cancer behaviours, such as the VEGF-Flt-1 pathway with invasion [9], kallikrein-related peptidase with metastatic capacity [10], and glutathione-peroxidase-I overexpression with poor prognosis [11]. None of these are yet in clinical use.

Nano Ultra-Performance Liquid Chromatography Label-Free Ultra-Definition Mass Spectrometry (nUPLC-UDMS^E) is a highly sensitive form of mass spectrometry (MS), capable of quantifying hundreds-to-thousands of proteins in solution. nUPLC-UDMS^E discovery-driven analysis offers a unique avenue to discover proteins and pathways that are previously not known to be altered in OSCC. Previously, studies using non-pooled paired healthy and OSCC tissue samples for direct comparison with MS have used a gel-based matrix to register the differences between the cases and controls after which protein spots are identified using MS [12–14]. However, shotgun proteomics, as done here, and the electrophoresis approaches have different scopes and limitations. Electrophoresis mainly homes in on critical alterations such as isoform differences, and post-translational modifications, whereas shotgun approaches aim for a broad overview of proteomic changes, including those with smaller abundances, and allows for novel protein discovery. These two approaches can be complementary [15].

The primary aim of this study was to identify and quantify the differences between healthy tissue and OSCC using nUPLC-UDMS^E proteomics. In particular, we aimed to discover novel proteins with significantly different expression in OSCC compared with controls, along with differences in protein expression between high- and low-grade tumours. This will facilitate future research to assess whether these proteins can be used as potential new prognostic or predictive biomarkers, for example predicting different clinical behaviours of OSCCs. Additionally, the discovery of proteins involved can help in identifying important pathways in OSCC pathogenesis and thus potential therapeutic targets.

Materials and methods

Briefly, tissues of primary OSCC of the mobile tongue, and paired healthy tongue epithelium were taken preoperatively and immediately frozen. At the time of analysis, the tissues were thawed and lysed, and protein extraction was performed. The proteins were trypsin digested, and the tryptic peptide mixture was analysed using mass spectrometry (nUPLC-UDMS^E), to identify proteins differing between OSCC and paired healthy epithelium. Statistical classification and separation techniques were performed to ensure clear differences between OSCC and healthy tissue. Pathway analysis using two methods were performed to assess altered pathways within OSCC to gain greater understanding. We additionally performed a comparison between stage I and stage IVa OSCC. Selected proteins that have previously been found to be altered in serum of OSCC [16,17] and that we also found to be altered in the tissue were validated with immunohistochemistry (IHC). A tissue microarray block of 66 patients with oral tongue OSCC was used for this IHC analysis. Patient and tumour information is in Supplementary Table 1. Detailed information about the materials and methods are found in Supplementary File 1. The workflow can be visualised in Fig. 1.

Ethical approval was granted by the institutional Research Ethics Committee at the Helsinki University Hospital (Dnro: 64/13/03/02/2014). All patients provided informed written consent to participate in the study.

Results

Proteomics of OSCC and healthy tongue tissue

Of 829 proteins with two or more unique peptides that were quantified, 257 proteins were statistically significant (Supplementary Table 2).

The majority of proteins were present in both the cancer and control tissue in differing amounts, but one protein (alpha-taxilin) was absent

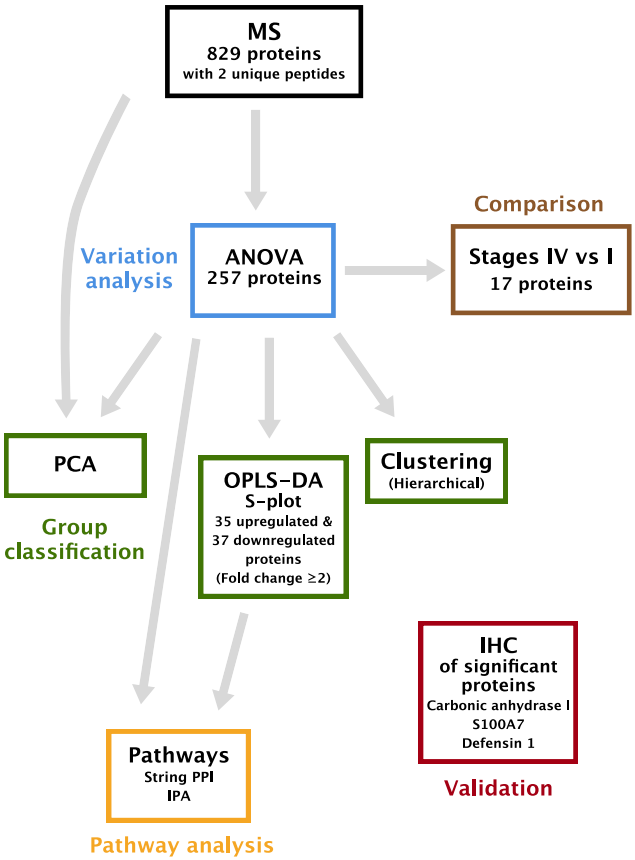

Fig. 1. Overview of methods employed, and results obtained. Mass spectrometry using nUPLC-UDMS^E (Nano Ultra Performance Liquid Chromatography Label Free Ultra-definition mass spectrometry was performed on OSCC of the tongue and paired healthy controls. Anova analysis was performed on these, with a p-value cut-off of 0.05. For group classification, PCA, OPLS-DA and Hierarchical Clustering Analysis were used, and significant proteins were identified using OPLS-DA analysis. Using String PPI and IPA, pathways altered in OSCC were identified. Furthermore, stage IVa vs stage I OSCC protein expressions were compared. Validation was performed on selected proteins, to confirm their presence is consistent in tumour samples, and to identify which cells within the tumour express these proteins. These proteins are known to be significantly altered in OSCC serum compared to controls in a previous study [16]. Key: ANOVA - Analysis of Variance; IHC – immunohistochemistry; IPA - Ingenuity Pathways Analysis; MS - mass spectrometry; OPLS-DA - Orthogonal Projections to Latent Structures Discriminant Analysis; PCA - Principal Component Analysis; String PPI - Protein-protein Interaction (via String).

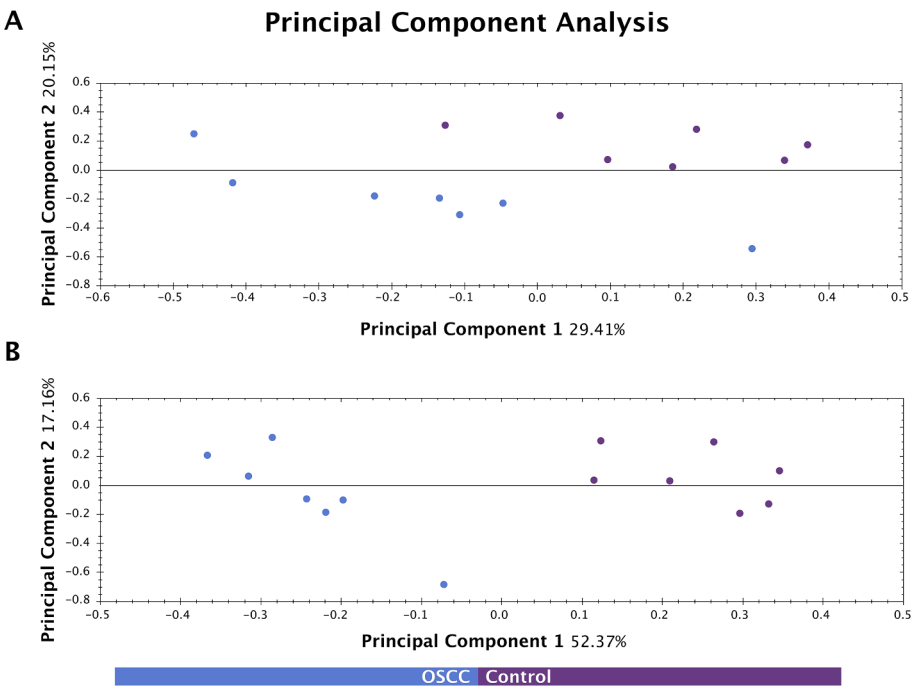

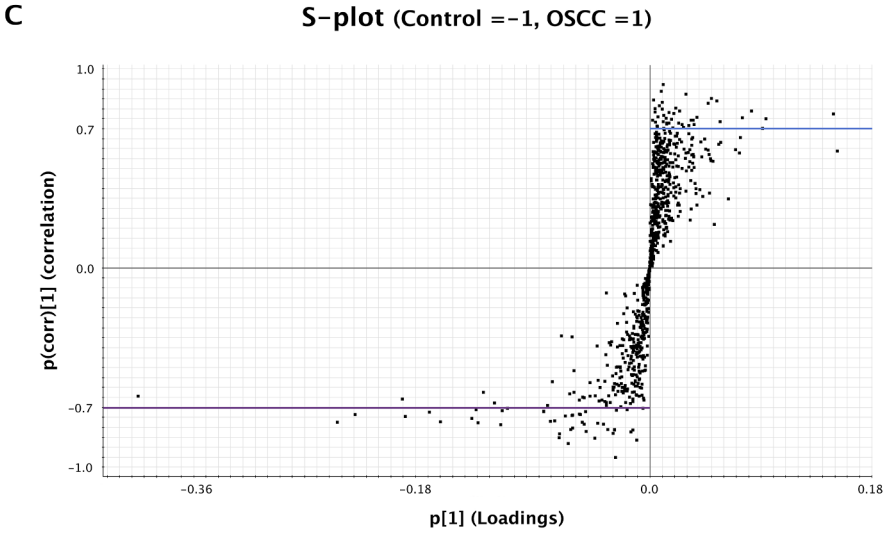

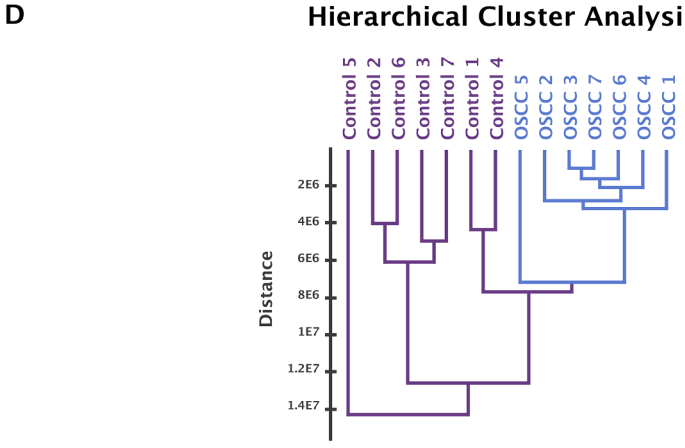

Fig. 2. Separation between the OSCC proteins demonstrated with three different methods. Principal Component Analysis when all the proteins (two or more unique peptides) were considered is shown in Panel A. Principal Component Analysis, when using proteins passing Anova cutoff p-value of 0.05, is shown in Panel B. Visualisation of OPLS-DA (Orthogonal Projections to Latent Structures Discriminant Analysis) modelling by S-plot, gave us the significantly different proteins, which could classify the OSCC from healthy tissue, is shown in Panel C. The upper right quadrant (with positive values) show proteins upregulated in OSCC tongue tissue; the lower left quadrant (with negative values) shows the proteins upregulated in the healthy tongue tissue. The cut-off used to separate significantly different proteins from other proteins was ± 0.7. The blue line represents the cut-off for proteins upregulated in OSCC, the purple line represents the cut-off for proteins downregulated in OSCC. Hierarchical clustering, using the Euclidean Similarity Index, shows branching between the OSCC and paired healthy tissue based on protein expression (Panel D). (For interpretation of the references to colour in this figure legend, the reader is referred to the web version of this article.)

in 5 of the 7 control samples, with low levels in the other two samples. Other highly upregulated proteins include neutrophil defensin 1 (DEFA1), and sickle tail protein homologue (KIAA1217), with mean fold changes (FC) of 18.2 and 18, respectively.

For confirmation of the separation and for further filtering of the proteins differing between the OSCC and healthy control tissue samples, various supervised and unsupervised statistical analyses were employed: Principal Component Analysis (PCA); Orthogonal Projections to Latent Structures Discriminant Analysis (OPLS-DA); Hierarchical Clustering Analysis (HCA). In all three of these analyses there was a clear separation between the OSCC and control tissues. HCA showed separate branches of OSCC and healthy samples based on protein abundances (Fig. 2d).

PCA was used to determine and visualise the principal axes of protein abundance variation between the two groups. This showed a complete separation between cancer and healthy tissue when using all 829 proteins, with the separation becoming even clearer when just the statistically significant proteins were included (Fig. 2a and b).

OPLS-DA was used to model the differences between the two groups. One OSCC tissue sample from patient number two was removed as it lay beyond the 95% confidence range. An S-plot was generated from the data (Fig. 2c). Proteins exceeding the p(corr) cut-off value of ± 0.7 were considered to be significant (Table 1). 35 upregulated and 37 downregulated proteins with FC of 2 or more were found in this s-plot, such as DEFA1 (FC 19.8; p(corr) 0.84), S100A7 (FC 5.1; p(corr) 0.85), carbonic anhydrase 1 (CA1) (FC 3.3; p(corr) 0.92). of these S-plot proteins had an area under the receiver operating characteristic curve (AUROC) of 1.0.

Comparison between proteomic signatures of the stage I and stage IVa OSCC

The proteomic differences between stage I and stage IVa OSCC were performed using the same methods as for the tumours versus controls. There were 17 protein differences with Anova $p < 0.05$, which can be seen in Table 2. The most upregulated of these being KIAA1217 (FC 4.94) and NDRG1 (FC 4.12). The most downregulated proteins were cytochrome b-c1 complex (FC -2.64) and heat shock protein HSP 90 alpha (FC -2.61). There was some overlap on PCA when using all the 827 proteins (Fig. 3a), however upon using the statistically significant proteins, there was a clear separation between stage I and stage IVa (Fig. 3b).

Immunohistochemistry of carbonic anhydrase 1 (CA1), S100A7, and neutrophil defensin 1 (DEFA1)

CA1, S100A7 and DEFA1 were proteins, which were also found to be altered in the serum of OSCC patients [17], as well being some of the most differentiating tissue proteins after OPLS-DA modelling. IHC of these proteins was performed on an independent tissue microarray (TMA) block cohort of OSCCs, and separate healthy tissue samples from OSCC patients. This confirmed stronger staining in OSCC than healthy epithelium. S100A7 showed heterogeneous cytoplasmic, membranous and nuclear positivity in tumour tissue, whereas in the controls positivity was present in only the epithelial keratin layer. DEFA1 immunopositivity was strong in tumour cells, both cytoplasm and nuclei, and additional positivity was detected in inflammatory cells surrounding the cancer tissue. In the control tissue, positivity was cytoplasmic throughout the epithelium, with more intense, and additional membranous positivity in the basal cell layers. CA1 showed moderate cytoplasmic positivity throughout the tumour tissue, and also membranous positivity in some tumours. Inflammatory cells also had immunopositivity. In the controls, positivity was localised to the epithelium, and was stronger in the basal layer. Fig. 4 shows examples of, and the proportions of mild, moderate and strong tumour staining positivity by intensity in the tumour.

Pathway analysis of OSCC tissue

We performed two analytical methods to determine the important networks and pathways altered in OSCC compared to healthy tissue. String protein–protein interactions (PPI) shows direct connections linking the S-plot proteins as shown in Fig. 5, where there are clusters of cytoskeletal proteins such as myosin and tropomyosin chains, and clusters of nuclear proteins such as ALYREF (THO complex subunit 4), NAP1L1 (nucleosome assembly protein 1-like 1), PABPN1 (Polyadenylate-binding protein 2), DNAJC8 (dnaJ homolog subfamily C member 8). Ingenuity pathway analysis (IPA) shows the significantly altered networks in OSCC, i.e. those enriched in the S-plot proteins. IPA includes proteins via which these proteins are known to interact, thus filling in the gaps of the proteins that may not have been detected. The top networks enriched were 1: 'Cellular movement, haematological system development and function, immune cell trafficking', 2: 'Hereditary disorder, organismal injury and abnormalities, skeletal and muscle disorders, 3: 'Cell-to-cell signalling and interaction, cellular movement, nervous system development and function', 4: 'Infectious diseases, dermatological diseases and condition, organismal injury and abnormalities'. These are all significant and highly enriched networks, with network scores between 31 and 56, and enriched with 16 to 25 proteins. This method verifies the s-plot proteins' significance on a pathway level. The overlay of both network analysis methods further shows that there is crossover between all of these OSCC networks. For example, a connection between ALYREF (THO complex subunit 4) and DNAJC8 connects Networks 2 and 3, connections between stathmin 1 (STMN1) and tropomyosins (connecting Networks 1 and 2).

IPA also identified significant canonical pathways enriched with the $p < 0.05$ proteins (Supplementary Fig. 1). The top canonical pathways include calcium signalling, regulation of actin-based motility by Rho, actin cytoskeleton signalling and tight junction signalling.

Discussion

OSCC is often detected late with the consequences of poor survival. Treatment can also be functionally impairing. OSCC incidence is increasing and has a high recurrence rate [6]. The disease course is unpredictable, without any established biomarkers for prognostication or prediction. Such biomarkers are needed urgently. Additionally, it is imperative to uncover the pathobiology of OSCC at the tissue level to identify potential treatment targets.

Proteomic comparisons

nUPLC-UDMS^{E} discovery-driven analysis offers a unique avenue to discover proteins and pathways that are previously not known to be altered in OSCC. Some similar patterns were found, when compared to previous proteomic studies [12–14] such as proteasome activator, peripherin, keratin (KRT) 17 and cofilin-1 upregulation [12], downregulation of cytoskeletal proteins such as myosin light and heavy chains, tropomyosins (except upregulation of tropomyosin 4) [14], and upregulation of matrix-metalloproteinase 9, S100A7, thymosin beta 10, tenascin C, calreticulin, and downregulation of lumican [18].

The 257 proteins significantly differing between OSCC and healthy tissue were further modelled using OPLS-DA, which classifies samples based on their protein signature and shows their separation and similarities in a way that is difficult to obtain using other means. Among the S-plot proteins generated from this analysis (Table 1), there were 19 proteins, which to our knowledge are not previously known to be upregulated in OSCC, although some have been found in other cancers. These could be further studied as potential biomarkers. Those with the greatest abundance include prosaposin (PSAP) and Acidic leucine-rich nuclear phosphoprotein 32 family member B (ANP32B). The rest are found in Table 1, along with p-value, fold change and AUROC information. ANP32B, with an AUROC of 0.939, is upregulated in

Table 1
The significant proteins obtained from an OPLS-DA (Orthogonal Projections to Latent Structures Discriminant Analysis) S-plot with a p(corr) cut-off of +/−0.7, of OSCC compared to healthy controls, are shown here. Proteins are sorted from the highest to lowest p(corr) values. Table heading explanations: UniProt: UniProt accession number; Gene name: the gene name, retrieved from UniProt; Protein name: the recommended name of the protein; All peptides: total number of identified peptides from the protein in our study; Unique peptides: the number of peptides, unique to the protein found, identified in our study; Anova p-value: the p-value calculated using Anova; AUROC: the area under the receiver operating characteristic curve; AUROC 95% CI: 95% confidence interval of the AUROC value; Fold change: mean fold change of the protein values, when comparing cancer to healthy tissue; p[1]: S-plot protein loading; p(corr): correlation coefficient. Where there are multiple uniport accession numbers for a protein, it represents the grouping of proteins, explained in Supplementary File 1 (page 3, line 21). Novel upregulated proteins in OSCC tissue are shown in bold.

UniProt	Gene name	Protein name	All peptides	Unique peptides	Anova p-value	AUROC	AUROC 95% CI	Fold change	p[1]	p(corr) [1]
P00915	*CA1*	Carbonic anhydrase 1	8	8	9.11E-04	1.00	–	3.3	0.01	0.92
Q86U42	***PABPN1***	**Polyadenylate-binding protein 2**	**5**	**2**	**4.99E-04**	**1.00**	**–**	**3.1**	**0.01**	**0.89**
Q01105;P0DME0	*SET*	Protein SET	24	17	1.72E-03	0.96	0.83–1	1.9	0.03	0.87
P31151	*S100A7*	Protein S100-A7	31	14	6.58E-03	0.96	0.84–1	5.1	0.05	0.85
A0A0B4J269	*N/A*	Uncharacterized protein	16	2	5.60E-03	1.00	–	3.1	0.00	0.84
P59665;P59666	*DEFA1*	Neutrophil defensin 1	8	7	1.79E-03	1.00	–	19.8	0.05	0.84
Q96K17	***BTF3L4***	**Transcription factor BTF3 homolog 4**	**3**	**2**	**1.37E-04**	**0.92**	**0.74–1**	**4.6**	**0.01**	**0.83**
P63313	*TMSB10*	Thymosin beta-10	5	4	1.07E-02	1.00	–	3.6	0.05	0.83
Q8N6V9	***TEX9***	**Testis-expressed sequence 9 protein**	**3**	**2**	**2.07E-03**	**0.98**	**0.90–1**	**3.9**	**0.01**	**0.81**
P67809	*YBX1*	Nuclease-sensitive element-binding protein 1	8	4	9.35E-03	0.96	0.84–1	4.3	0.02	0.80
Q86SG5	*S100A7A*	Protein S100-A7A	15	2	1.32E-02	0.96	0.84–1	18.3	0.00	0.80
Q15468	***STIL***	**SCL-interrupting locus protein**	**3**	**3**	**7.25E-03**	**0.96**	**0.84–1**	**4.8**	**0.01**	**0.80**
Q9Y2V2	***CARHSP1***	**Calcium-regulated heat-stable protein 1**	**8**	**6**	**3.01E-03**	**0.94**	**0.80–1**	**2.4**	**0.02**	**0.79**
P27797	*CALR*	Calreticulin	47	38	9.26E-04	0.94	0.76–1	2.4	0.08	0.79
O75937	***DNAJC8***	**DnaJ homolog subfamily C member 8**	**5**	**2**	**2.02E-02**	**0.88**	**0.67–1**	**2.2**	**0.00**	**0.78**
Q96MG8	***PCMTD1***	**Protein-L-isoaspartate O-methyltransferase domain-containing protein 1**	**3**	**2**	**1.45E-02**	**0.96**	**0.84–1**	**1.8**	**0.02**	**0.78**
P55209	*NAP1L1*	Nucleosome assembly protein 1-like 1	15	11	1.13E-02	0.94	0.76–1	3.2	0.02	0.77
Q96AG4	*LRRC59*	Leucine-rich repeat-containing protein 59	3	2	1.10E-02	0.92	0.71–1	3.6	0.01	0.77
A6NDA9	***LRIT2***	**Leucine-rich repeat, immunoglobulin-like domain and transmembrane domain-containing protein 2**	**2**	**2**	**3.36E-02**	**0.86**	**0.60–1**	**2.7**	**0.01**	**0.76**
Q92688	***ANP32B***	**Acidic leucine-rich nuclear phosphoprotein 32 family member B**	**17**	**8**	**4.35E-03**	**0.94**	**0.76–1**	**2.1**	**0.04**	**0.76**
P67936	*TPM4*	Tropomyosin alpha-4 chain	63	18	6.36E-04	0.94	0.80–1	2.4	0.07	0.75
P53999	***SUB1***	**Activated RNA polymerase II transcriptional coactivator p15**	**5**	**4**	**1.45E-02**	**0.92**	**0.72–1**	**3.5**	**0.01**	**0.75**
P11021	*HSPA5*	78 kDa glucose-regulated protein	82	61	1.91E-04	0.94	0.76–1	1.9	0.09	0.75
P49321	***NASP***	**Nuclear autoantigenic sperm protein**	**24**	**21**	**4.72E-03**	**0.96**	**0.83–1**	**2.1**	**0.02**	**0.75**
P40222	***TXLNA***	**Alpha-taxilin**	**3**	**2**	**1.56E-03**	**1.00**	**–**	**26**	**0.00**	**0.74**
P80511	*S100A12*	Protein S100-A12	11	8	1.05E-02	1.00	–	5.1	0.03	0.74
P07602	***PSAP***	**Prosaposin**	**40**	**30**	**1.13E-04**	**0.98**	**0.88–1**	**2.5**	**0.06**	**0.73**
Q9NZZ3	*CHMP5*	Charged multivesicular body protein 5	3	2	1.55E-02	0.98	0.88–1	5.1	0.01	0.73
P35232	*PHB*	Prohibitin	5	2	3.62E-02	0.94	0.76–1	4	0.00	0.73
Q86V81	*ALYREF*	THO complex subunit 4	9	5	1.56E-03	0.96	0.88–1	2.4	0.02	0.73
O00515;P42766	*LAD1*	Ladinin-1	31	24	4.61E-03	1.00	–	1.5	0.02	0.73
P16949; Q93045	***STMN1***	**Stathmin**	**10**	**5**	**7.42E-03**	**0.94**	**0.76–1**	**2.1**	**0.01**	**0.73**
P04003	***C4BPA***	**C4b-binding protein alpha chain**	**5**	**4**	**7.82E-03**	**1.00**	**–**	**6.7**	**0.01**	**0.72**
O43399	*TPD52L2*	Tumor protein D54	10	5	4.85E-03	0.90	0.71–1	1.7	0.03	0.72
Q04695	*KRT17*	Keratin, type I cytoskeletal 17	56	20	1.36E-02	0.94	0.80–1	2	0.04	0.72
P29034	*S100A2*	Protein S100-A2	6	6	1.83E-02	0.86	0.64–1	2	0.03	0.71
Q8WWX9	***SELM***	**Selenoprotein M**	**3**	**2**	**7.88E-03**	**0.90**	**0.67–1**	**3.3**	**0.01**	**0.71**
Q9P0L0	***VAPA***	**Vesicle-associated membrane protein-associated protein A**	**7**	**4**	**5.08E-03**	**0.90**	**0.66–1**	**2.2**	**0.01**	**0.71**
P30040	***ERP29***	**Endoplasmic reticulum resident protein 29**	**22**	**16**	**4.98E-03**	**0.94**	**0.74–1**	**1.8**	**0.03**	**0.70**
P54727	*RAD23B*	UV excision repair protein RAD23 homolog B	10	5	1.24E-02	0.94	0.76–1	2.4	0.02	0.70
O14879	***IFIT3***	**Interferon-induced protein with tetratricopeptide repeats 3**	**9**	**5**	**5.80E-03**	**0.98**	**0.88–1**	**9.2**	**0.01**	**0.70**
P07585	*DCN*	Decorin	40	31	3.03E-03	1.00	–	−4.6	−0.12	−0.70
Q5BKX8	*MURC*	Muscle-related coiled-coil protein	2	2	1.58E-03	1.00	–	−36.9	−0.01	−0.71
P02585	*TNNC2*	Troponin C, skeletal muscle	48	41	1.06E-03	1.00	–	−11.5	−0.14	−0.71
P09493	*TPM1*	Tropomyosin alpha-1 chain	74	26	6.71E-03	1.00	–	−5.4	−0.12	−0.72
P13646	*KRT13*	Keratin, type I cytoskeletal 13	61	31	1.24E-04	1.00	–	−6.2	−0.09	−0.72
P51888	*PRELP*	Prolargin	27	24	8.04E-04	1.00	–	−5.7	−0.09	−0.72
O75112	*LDB3*	LIM domain-binding protein 3	17	12	8.01E-03	0.98	0.92–1	−5.3	−0.05	−0.72
P04083	*ANXA1*	Annexin A1	98	74	5.83E-04	1.00	–	−2.8	−0.18	−0.73
P20774	*OGN*	Mimecan	30	26	1.31E-03	1.00	–	−5.9	−0.06	−0.73
P05976	*MYL1*	Myosin light chain 1/3, skeletal muscle isoform	77	55	6.70E-04	1.00	–	−12.3	−0.24	−0.74
Q9UKX2	*MYH2*	Myosin-2	127	33	1.17E-02	0.94	0.77–1	−2.1	−0.06	−0.74
P00568	*AK1*	Adenylate kinase isoenzyme 1	27	15	2.16E-03	1.00	–	−3.8	−0.06	−0.74

(*continued on next page*)

Table 1 (*continued*)

UniProt	Gene name	Protein name	All peptides	Unique peptides	Anova p-value	AUROC	AUROC 95% CI	Fold change	p[1]	p(corr) [1]
P31415	*CASQ1*	Calsequestrin-1	23	14	2.94E-04	1.00	–	−16.3	−0.07	−0.74
Q9UBG3	*CRNN*	Cornulin	55	46	1.21E-04	1.00	–	−5.4	−0.20	−0.75
P07951	*TPM2*	Tropomyosin beta chain	83	28	9.48E-04	1.00	–	−3.9	−0.14	−0.76
P06753	*TPM3*	Tropomyosin alpha-3 chain	67	25	3.25E-03	0.98	0.88–1	−2.5	−0.08	−0.77
P51884	*LUM*	Lumican	49	35	5.83E-03	1.00	–	−3.6	−0.17	−0.77
P48788	*TNNI2*	Troponin I, fast skeletal muscle	19	11	1.19E-03	1.00	–	−5.4	−0.05	−0.77
P02144	*MB*	Myoglobin	71	59	1.31E-04	1.00	–	−21.5	−0.25	−0.78
P10916	*MYL2*	Myosin regulatory light chain 2, ventricular/cardiac muscle isoform	54	35	3.72E-04	1.00	–	−6.7	−0.14	−0.78
Q15847;Q9BZL4	*ADIRF*	Adipogenesis regulatory factor	8	6	1.01E-03	1.00	–	−4.9	−0.04	−0.78
Q6NZI2	*PTRF*	Polymerase I and transcript release factor	22	16	1.17E-02	0.96	0.82–1	−2.2	−0.04	−0.78
Q9BUF5	*TUBB6*	Tubulin beta-6 chain	14	6	2.26E-03	0.94	0.74–1	−5.8	−0.05	−0.79
P08590	*MYL3*	Myosin light chain 3	39	26	5.86E-04	0.98	0.88–1	−11.6	−0.12	−0.79
P17661	*DES*	Desmin	69	44	8.52E-04	1.00	–	−3.3	−0.06	−0.81
Q16610	*ECM1*	Extracellular matrix protein 1	14	14	1.21E-04	0.98	0.92–1	−3.7	−0.03	−0.81
P40926	*MDH2*	Malate dehydrogenase, mitochondrial	16	11	2.30E-02	0.92	0.76–1	−1.9	−0.03	−0.81
P30086	*PEBP1*	Phosphatidylethanolamine-binding protein 1	22	17	6.30E-04	1.00	–	−2.2	−0.06	−0.81
Q9HCY8	*S100A14*	Protein S100-A14	13	10	1.38E-03	1.00	–	−2.9	−0.03	−0.81
Q8N1N4	*KRT78*	Keratin, type II cytoskeletal 78	11	5	3.91E-03	0.96	0.84–1	−2.8	−0.01	−0.81
Q9NQ38	*SPINK5*	Serine protease inhibitor Kazal-type 5	57	35	7.72E-05	0.94	0.80–1	−2.4	−0.05	−0.82
P13805	*TNNT1*	Troponin T, slow skeletal muscle	7	5	1.29E-04	1.00	–	−5.8	−0.02	−0.82
P02511	*CRYAB*	Alpha-crystallin B chain	12	9	1.32E-05	1.00	–	−9.8	−0.03	−0.83
P14174	*MIF*	Macrophage migration inhibitory factor	10	7	1.85E-03	0.94	0.76–1	−2.2	−0.07	−0.83
P19013;P14136; Q6KB66	*KRT4*	Keratin, type II cytoskeletal 4	50	32	5.23E-04	1.00	–	−3.3	−0.07	−0.85
P14649	*MYL6B*	Myosin light chain 6B	26	17	5.63E-05	0.98	0.88–1	−4.8	−0.04	−0.86
Q12836	*ZP4*	Zona pellucida sperm-binding protein 4	2	2	1.52E-02	0.86	0.57–1	−2.6	−0.01	−0.87
O60437;P80217	*PPL*	Periplakin	104	59	1.16E-04	1.00	–	−1.9	−0.07	−0.88
O15231	*ZNF185*	Zinc finger protein 185	20	13	1.36E-04	1.00	–	−2.6	−0.03	−0.95

colorectal carcinoma [19] and breast cancer, and knockdown in cancer cells induced G1 arrest [20]. Alpha-taxilin, with an AUROC of 1, is interesting through its absence in 5 of the 7 control samples. It has not been found in OSCC before, but in colorectal cancer its overexpression correlates with proliferation activity [21], and is associated with metastatic and invasive potential of renal cell carcinoma [22]. These may be of interest for future research in OSCC.

The two most upregulated proteins in stage IVa tumours, compared with stage I (Table 2), were KIAA1217 and protein NDRG1, both linked with proto-oncogenes. Little is known of KIAA1217 in cancer. It was recently discovered as a novel fusion partner gene with the RET proto-oncogene in one case of lung adenocarcinoma, whereby the fusion of RET with KIAA1217 led to activation of downstream signalling molecules: STAT3, AKT, and ERK. This was linked with increased tumour cell invasion in the study [23]. However, there are no further studies or reports of this protein in carcinoma progression. Also known as n-myc downstream-regulator protein 1, NDRG1 is a metastasis suppressor gene that inhibits the NF-κB (nuclear factor-κB) pathway, thus inhibiting functions such as angiogenesis, proliferation, migration and invasion [24]. Its over-expression in OSCC has been linked in one study with long-term specific survival [25]. As the n numbers were small in our study, with three stage I and four stage IVa tumours, more investigation will be required to validate these results, especially with regards to the relatively unknown KIAA1217.

Three of the most significantly different proteins in the tissue proteomic analysis found on S-plot, that were also altered in serum OSCC compared to healthy [16], were S100A7, DEFA1 and CA1.

CA1 has been discovered in other tumours, such as breast cancer and small cell lung cancer (SCLC). In breast cancer, CA1 blockade with siRNA in tumour cell lines stimulated apoptosis and cell migration, suggesting that it may have an important role in mediating these processes [26]. Its upregulation in SCLC serum compared with benign lung disease patients, and healthy controls, caused it to be suggested as a potential biomarker [27]. Carbonic anhydrases are downstream proteins of hypoxia-inducible factor, which becomes stabilised under hypoxic conditions, for example in tumour cells, and mediates the transcription of proteins involved in glycolysis, angiogenesis and pH regulation [28]. Levels of CA1 in our study had a fold change of 3.4 in the tissue, compared with healthy samples. In the tumour tissue, CA1 immunopositivity was stronger than in controls. It has recently shown a similar upregulation in OSCC tissue using electrophoresis-based proteomics [14]. Other carbonic anhydrase family members IX and XII have been extensively investigated in cancers, including CAIX in OSCC [29]. There are some promising carbonic anhydrase inhibitors; phase 1 trials are currently underway for the selective carbonic anhydrase IX inhibitor SLC-0111 in patients with advanced solid tumours [30].

DEFA1 is produced by epithelial cells and neutrophils, and has been identified in multiple carcinomas, including overexpression in human oral tongue OSCC [31]. Another previous tongue OSCC study, which showed an association between neutrophil invasion and lymph node metastasis, higher stage, and increased rate of tumour recurrence, also demonstrated strong DEFA1 immunopositivity in neutrophils within tumour tissue but not in the surrounding tissue [32]. That study showed high protein fold changes in OSCC compared with control, similar to our fold change of 19.8 found with MS. In our study, IHC demonstrated DEFA1 immunopositivity in both inflammatory cells and tumour cells. Mild to moderate positivity was also seen in normal epithelia, however no particular staining of inflammatory cells in the control samples.

S100 proteins are known to be involved in tumours; some members as tumour suppressors and others act as tumour promotors [33]. S100A7 is a key player in tumour migration, invasion and induction of epithelial-mesenchymal transition, among others in OSCC [34]. In our study, S100A7

Table 2
Proteomic comparison between OSCC tissue, stage I and stage IVa. Table of significant up- (in bold) and downregulated proteins in stage IVa cancers compared with those in stage I cancers. The proteins have been sorted according to fold change, which ranges from 1.51–4.94 in the proteins upregulated in stage IVa, and 1.5–2.6 in the proteins downregulated in stage IVa, compared to stage I OSCC. Heading explanations: UniProt: UniProt accession number; Gene name: the gene name, retrieved from UniProt; Protein name: the recommended name of the protein; All peptides: total number of identified peptides from the protein in our study; Unique peptides: the number of peptides, unique to the protein found, identified in our study; Anova p-value: the p-value calculated using Anova; Fold change: mean fold change of the protein values, when comparing stage IVa to Stage I. Where there are multiple uniport accession numbers for a protein, it represents the grouping of proteins, explained in Supplementary File 1 (page 3, line 21).

UniProt	Gene name	Protein name	All peptides	Unique peptides	Anova p-value	Fold change
Q5T5P2	***KIAA1217***	**Sickle tail protein homolog**	**4**	**2**	**0.021171**	**4.938**
Q92597	***NDRG1***	**Protein NDRG1**	**13**	**12**	**0.020015**	**4.124**
P23434	***GCSH***	**Glycine cleavage system H protein, mitochondrial**	**8**	**3**	**0.047383**	**1.542**
Q01105;P0DME0	***SET***	**Protein SET**	**24**	**17**	**0.024139**	**1.513**
P07919;A0A096LP55	*UQCRH*	Cytochrome b-c1 complex subunit 6, mitochondrial	9	9	0.047026	−2.646
Q14568	*HSP90AA2P*	Heat shock protein HSP 90-alpha A2	13	5	0.000494	−2.612
P04259	*KRT6B*	Keratin, type II cytoskeletal 6B	73	2	0.030769	−2.201
Q16610	*ECM1*	Extracellular matrix protein 1	14	14	0.042774	−2.154
P06702	*S100A9*	Protein S100-A9	76	65	0.014422	−2.049
O43768;P56211	*ENSA*	Alpha-endosulfine	7	5	0.049813	−1.969
P13284	*IFI30*	Gamma-interferon-inducible lysosomal thiol reductase	6	4	0.025037	−1.959
Q9Y281	*CFL2*	Cofilin-2	17	3	0.044786	−1.903
Q9HCY8	*S100A14*	Protein S100-A14	13	10	0.026441	−1.832
P15311	*EZR*	Ezrin	43	15	0.006186	−1.767
P07951	*TPM2*	Tropomyosin beta chain	83	28	0.006667	−1.67
Q9H3N1	*TMX1*	Thioredoxin-related transmembrane protein 1	2	2	0.018378	−1.623
Q96FQ6	*S100A16*	Protein S100-A16	8	7	0.007353	−1.545

expression was detected in all tumour samples. Interestingly, there was heterogeneity in positivity in the tumour tissue, shown in Fig. 4. In head and neck squamous cell carcinoma (HNSCC), nuclear S100A7 has been associated with reduced disease-free survival [35]. Members of the S100 protein family are differently expressed in various cancers – expression patterns depend on the tumour, its subtype and stage [33]. In HNSCC, the majority of the S100 proteins are downregulated whereas in most other cancers they tend to be upregulated (33), contrasting with our findings of

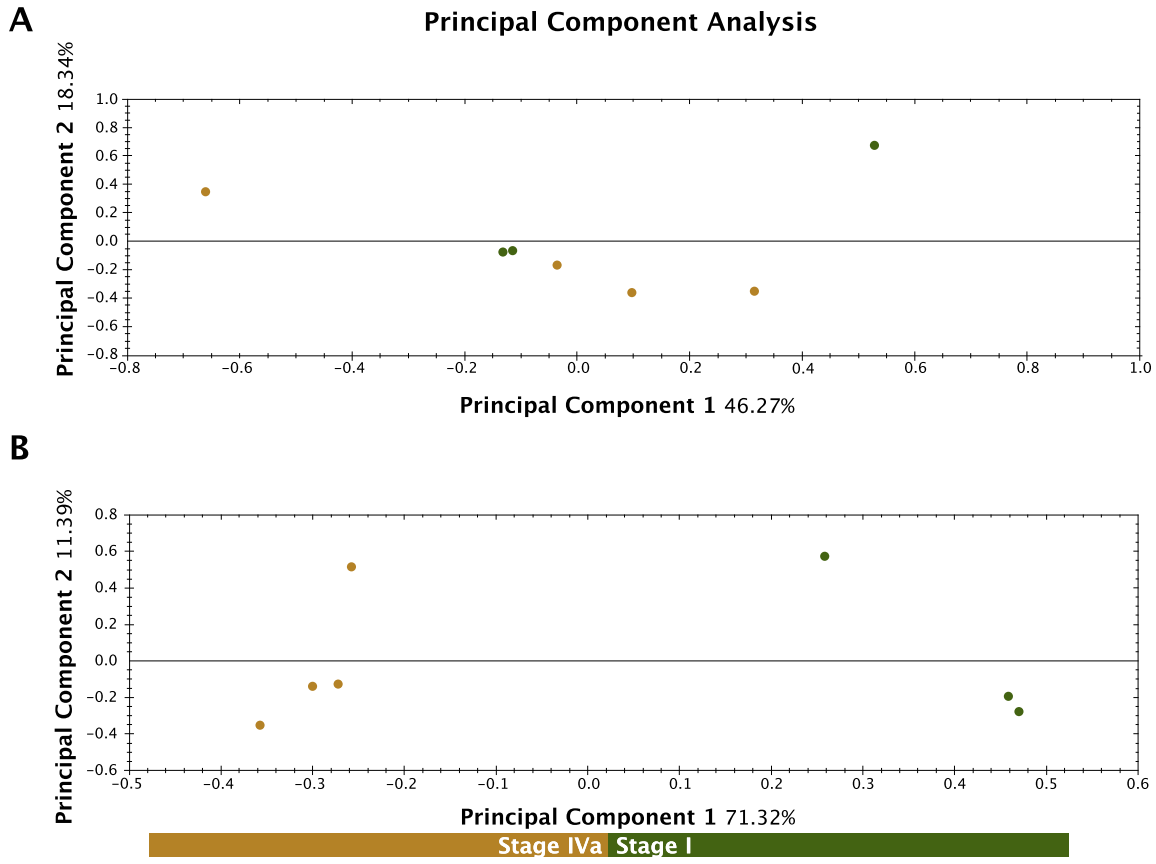

Fig. 3. Separation between the stage IVa compared to stage I samples using Principal Component Analysis (PCA). A: PCA of stage I and stage IVa samples, when expression of all proteins with two or more unique peptides were considered, is shown here. B: PCA when all proteins passing the cut-off of Anova p-value 0.05, is shown here.

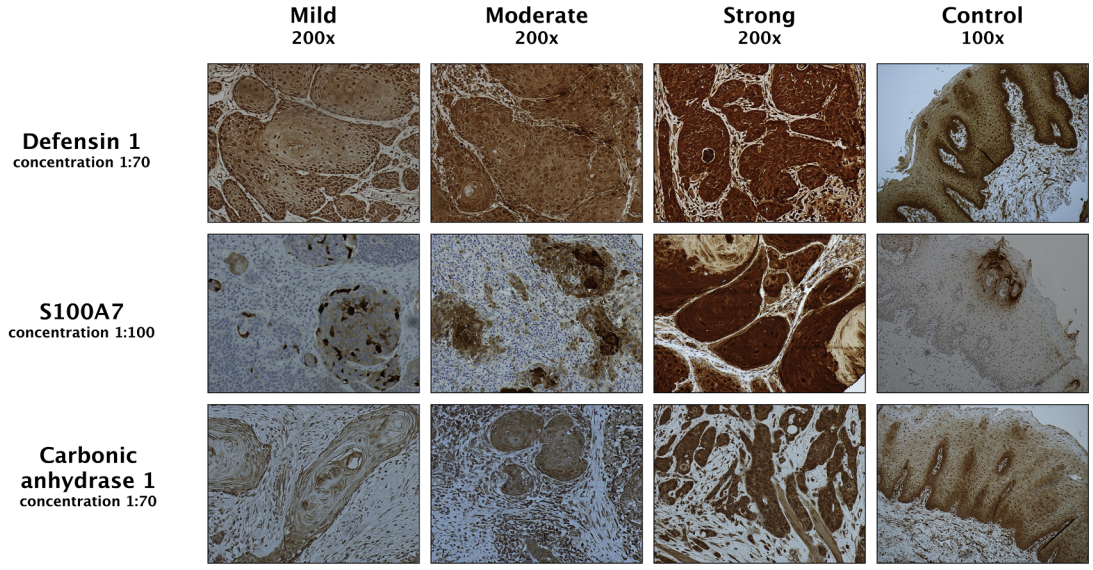

	Negative	Mild	Moderate	Strong
Defensin 1 n=66	0	1 1.5 %	15 22.7 %	50 75.6 %
S100A7 n=65	1 1.5 %	4 6.2 %	24 36.9 %	36 55.4 %
Carbonic anhydrase 1 n=66	0	4 6.1 %	47 71.2 %	15 22.7 %

Fig. 4. Immunohistochemistry of S100A7, neutrophil defensin 1, and carbonic anhydrase 1. The top composite image shows immunohistochemical staining patterns using: anti-defensin 1 antibodies (first row of images); anti-S100A7 antibodies (second row of images); anti-carbonic anhydrase 1 antibodies (third row) in the tumour samples at 200x magnification. Control images are on the right-hand panel at 100x magnification to show the whole epithelial layer. The images were taken with a Nicon Eclipse 80i microscope. Below the composite image are the numbers and percentage of tumours with different staining intensities for each antibody, expressed in a tabular format.

other S100 proteins S100A2, 7, 7A, 12 being significantly upregulated in the OSCCs, which could be the particular pattern in tongue cancer. Clinical trials are ongoing for targeting other S100 proteins, like S100B in melanoma [36], confirming that there is a possibility to target these proteins therapeutically.

Pathway analysis

One aim of our study was to gain insight into the pathways and networks upregulated in the tongue cancer compared with healthy tongue tissue from the same patient. The canonical pathways (Supplementary Fig. 1) involved in OSCC include calcium signalling, cell-to-cell interaction signalling, and immune system pathways involving phagocytes, amongst others.

Calcium signalling has a fundamental biological role, evolutionarily developed to be at the centre of almost all cellular processes, including signalling between cells, transcription, motility, innate immunity and apoptosis [37]. In cancer cells the calcium homeostasis is disrupted, as can be seen as the top canonical pathway involved. It is well established that calcium signalling alterations are implicated in tumour induction, angiogenesis, proliferation and metastasis [38]. Other examples of alterations are that, calcium-regulated membrane protein mutations, such as the IP3R (Inositol triphosphate receptor), have been detected in HNSCC [39], and the PMCA1 (plasma membrane Ca2 + ATPase isoform 1) calcium transporter expression has been found to be downregulated in OSCC [38]. In our samples, a handful of calcium related proteins were upregulated, including but not limited to calreticulin, calponin 1 and 3, reticulocalbin, S100 proteins, which were upregulated, and calsequestrin was downregulated.

The network most enriched with the S-plot proteins, suggesting the most disrupted networks, was 'Cellular Movement, Haematological System Development and Function, Immune Cell Trafficking', linking in with the calcium signalling and other top canonical pathways. This network was almost completely enriched in S-plot proteins (Fig. 5). It centres around NF-κB and MAPK (mitogen activated protein kinase), and contains multiple groups of proteins such as the S100s and the keratins amongst others. NF-κB plays a role in the regulation of various genes, including matrix metalloproteinases, anti-apoptotic factors, adhesion molecules, cytokines [40]. MAPKs are involved in the regulation of cell differentiation, proliferation and death in OSCC [41].

In addition to their important role in mechanical stability and structural integrity of epithelial cells, keratins have additional functions including protection from stress, wound healing and apoptosis [42]. Expression of keratin isoforms differs in various cancers, reflecting tumour activity, and they thus have the potential to serve as prognostic markers as fragments of the cytokeratins have been demonstrated in the circulation. The cytokeratin detection tests known as TPA, which measures cytokeratins 8, 18 and 19 in the serum, and CYFRA-1, which measures soluble cytokeratin 18 fragments, have been documented in various epithelial cell related tumours including head and neck cancers [43], as ways to monitor progression and response to treatment. KRT17 has been suggested as a diagnostic marker for OSCC and is highly

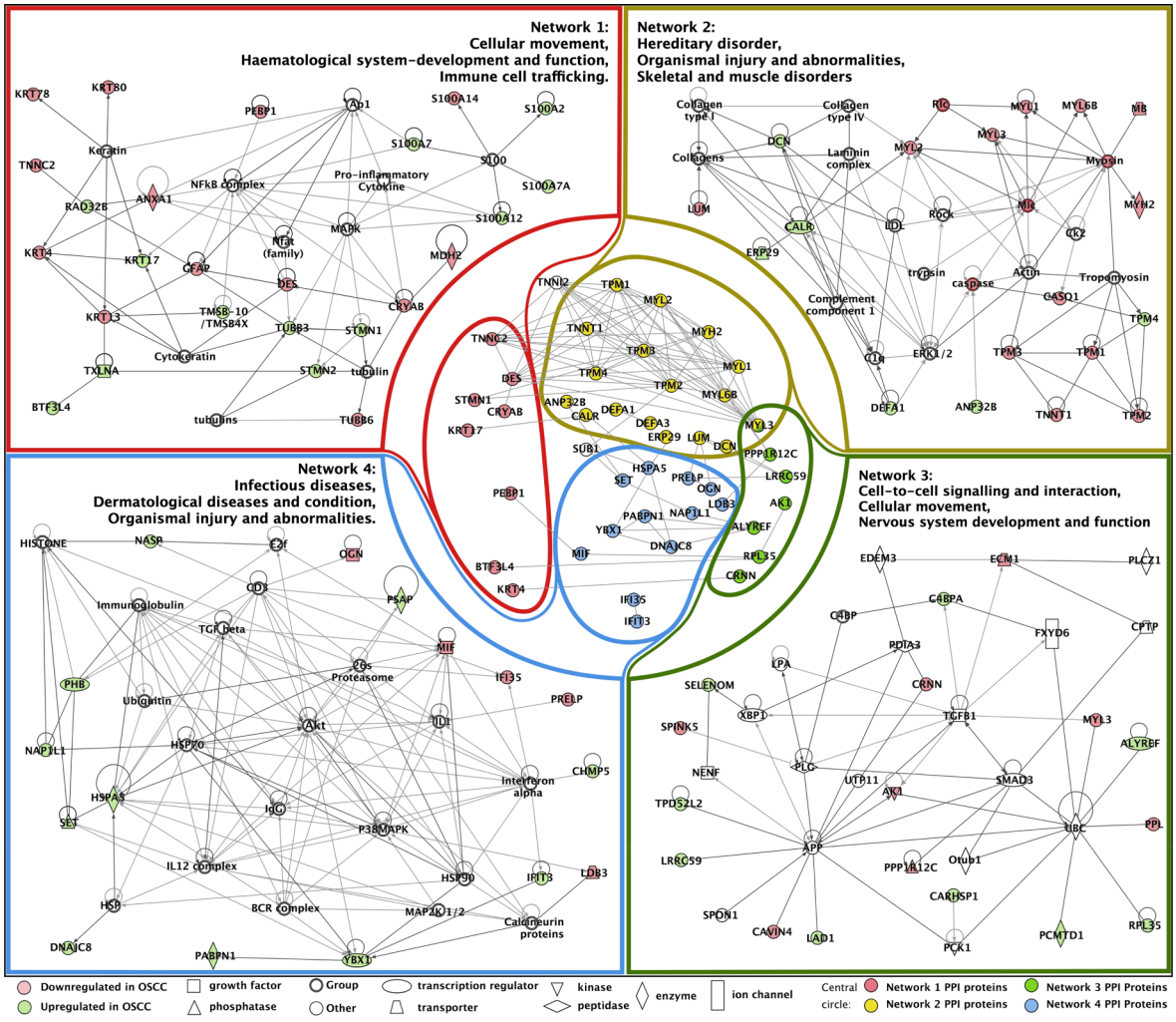

Fig. 5. Protein-protein interaction (PPI) networks of proteins found to be significantly different between OSCC tissue and healthy tissue by S-plot. The central circle shows PPI networks obtained using String. In each corner are the top four PPI networks obtained using Ingenuity Pathways Analysis (IPA), which also include proteins with which the proteins, identified in our study, are known to interact. The names of the networks are given in each rectangle. The coloured rings in the central area correspond to interactions, which were overlapping between String networks and IPA networks. In the corner boxes, corresponding to IPA networks, the proteins found in our study are coloured, and the key shows the function of each protein and whether it was upregulated or downregulated in OSCC. This diagram highlights the overlap between two different algorithms (IPA and String).

upregulated in the OSCC tissue on IHC [44]. In one study, KRT17 with low KRT13 was suggestive of malignant changes within oral lesions [45], which correlates with our results of downregulated KRT13 (FC -6.19) and upregulated KRT17 (FC 1.98) in the tumour tissue.

Conclusions

We have shown that based on tissue proteomics, tongue cancer tissue samples can be separated from samples of healthy adjacent tissue. With an MS technique, we were able to identify a set of 35 upregulated and 37 downregulated statistically relevant proteins that most reliably represent this separation, many of which were novel in OSCC. These proteins were found to participate in processes including calcium signalling, epithelial integrity, neutrophil functioning, and cellular movement. There were some overlapping proteins compared to previous proteomic analysis however several novel proteins were detected, such as alpha-taxilin. Additionally, we show that KIAA1217 and NDRG1 are upregulated in stage IVa OSCC compared with stage I. We need further research to clarify whether the expression of some of these key proteins could serve as a potential biological classification component of different OSCC tumours.

Availability of data and material

The datasets supporting the conclusions of this article are available in the ProteomeXchange repository, PXD009244 for tissue data and PXD005263 for serum data [16,17] http://proteomecentral.proteomexchange.org/cgi/GetDataset.

Conflicts of interest

None.

Acknowledgements

Thank you to Päivi Peltokengas for her contribution to the IHC wet lab, to Rayan Mroueh for his contribution to the TMA block patient information, and to Rahul Agarwal for his assistance with statistical analysis.

Funding was provided by Jane & Aatos Erkko Foundation, University of Helsinki Medical Faculty, and the Finnish Foundation for Ear, Nose and Throat Research (Korvatautien Tutkimussäätiö), and the Helsinki University Hospital Research Fund, who all supported the entire research from study design to manuscript writing, and Emil

Aaltonen Research Foundation, grant number (180025 N1) and Finnish-Norwegian Foundation for Medicine, grant number (201800155), who supported the revision of the manuscript.

Appendix A. Supplementary material

Supplementary data to this article can be found online at https://doi.org/10.1016/j.oraloncology.2018.09.013.

References

[1] Annertz K, Anderson H, Palmer K, Wennerberg J. The increase in incidence of cancer of the tongue in the Nordic countries continues into the twenty-first century. Acta Otolaryngol 2012;132(5):552–7.

[2] Chaturvedi AK, Anderson WF, Lortet-Tieulent J, Curado MP, Ferlay J, Franceschi S, et al. Worldwide trends in incidence rates for oral cavity and oropharyngeal cancers. J Clin Oncol 2013;31(36):4550–9.

[3] Braakhuis BJ, Leemans CR, Visser O. Incidence and survival trends of head and neck squamous cell carcinoma in the Netherlands between 1989 and 2011. Oral Oncol 2014;50(7):670–5.

[4] UK CR. Survival | Mouth (oral) cancer | Cancer Research UK: Cancer Research UK; 2016 [updated 06 July 2016. Available from: http://www.cancerresearchuk.org/about-cancer/mouth-cancer/survival.

[5] Siegel RL, Miller KD, Jemal A. Cancer statistics, 2016. CA Cancer J Clin 2016;66(1):7–30.

[6] Mroueh R, Haapaniemi A, Grenman R, Laranne J, Pukkila M, Almangush A, et al. Improved outcomes with oral tongue squamous cell carcinoma in Finland. Head Neck 2017;39(7):1306–12.

[7] Pathare SM, Gerstung M, Beerenwinkel N, Schaffer AA, Kannan S, Pai P, et al. Clinicopathological and prognostic implications of genetic alterations in oral cancers. Oncol Lett 2011;2(3):445–51.

[8] Blatt S, Kruger M, Ziebart T, Sagheb K, Schiegnitz E, Goetze E, et al. Biomarkers in diagnosis and therapy of oral squamous cell carcinoma: a review of the literature. J Craniomaxillofac Surg 2017;45(5):722–30.

[9] Subarnbhesaj A, Miyauchi M, Chanbora C, Mikuriya A, Nguyen PT, Furusho H, et al. Roles of VEGF-Flt-1 signaling in malignant behaviors of oral squamous cell carcinoma. PLoS ONE 2017;12(11):e0187092.

[10] Cui Z, Cui Y, Luo G, Yang S, Ling X, Lou Y, et al. Kallikrein-related peptidase 4 contributes to the tumor metastasis of oral squamous cell carcinoma. Biosci Biotechnol Biochem 2017;81(9):1768–77.

[11] Lee JR, Roh JL, Lee SM, Park Y, Cho KJ, Choi SH, et al. Overexpression of glutathione peroxidase 1 predicts poor prognosis in oral squamous cell carcinoma. J Cancer Res Clin Oncol 2017;143(11):2257–65.

[12] Chanthammachat P, Promwikorn W, Pruegsanusak K, Roytrakul S, Srisomsap C, Chokchaichamnankit D, et al. Comparative proteomic analysis of oral squamous cell carcinoma and adjacent non-tumour tissue from Thailand. Arch Oral Biol 2013;58(11):1677–85.

[13] Chen J, He QY, Yuen AP, Chiu JF. Proteomics of buccal squamous cell carcinoma: the involvement of multiple pathways in tumorigenesis. Proteomics 2004;4(8):2465–75.

[14] Ananthi S, Lakshmi CNP, Atmika P, Anbarasu K, Mahalingam S. Global quantitative proteomics reveal deregulation of cytoskeletal and apoptotic signalling proteins in oral tongue squamous cell carcinoma. Sci Rep 2018;8(1):1567.

[15] Oliveira BM, Coorssen JR, Martins-de-Souza D. 2DE: the phoenix of proteomics. J Proteomics 2014;104:140–50.

[16] Saraswat M, Makitie A, Agarwal R, Joenvaara S, Renkonen S. Oral squamous cell carcinoma patients can be differentiated from healthy individuals with label-free serum proteomics. Br J Cancer 2017;117(3):376–84.

[17] Saraswat MMA, Agarwal R, Joenvaara S, Renkonen S. Novel diagnostic biomarkers in serum identify patients with OSCC. Proteome Exchange Consortium; 2017. < http://proteomecentral.proteomexchange.org/cgi/GetDataset?ID=PXD005263 > .

[18] Dey KK, Pal I, Bharti R, Dey G, Kumar BN, Rajput S, et al. Identification of RAB2A and PRDX1 as the potential biomarkers for oral squamous cell carcinoma using mass spectrometry-based comparative proteomic approach. Tumour Biol 2015;36(12):9829–37.

[19] Uzozie AC, Selevsek N, Wahlander A, Nanni P, Grossmann J, Weber A, et al. Targeted proteomics for multiplexed verification of markers of colorectal tumorigenesis. Mol Cell Proteomics 2017;16(3):407–27.

[20] Yang S, Zhou L, Reilly PT, Shen SM, He P, Zhu XN, et al. ANP32B deficiency impairs proliferation and suppresses tumor progression by regulating AKT phosphorylation. Cell Death Dis 2016;7:e2082.

[21] Kanamori A, Imai Y, Ihara K, Nagata H, Nakano M, Tominaga K, et al. alpha-taxilin overexpression correlates with proliferation activity but not with prognosis of colorectal cancer. Oncol Lett 2017;14(2):1471–6.

[22] Mashidori T, Shirataki H, Kamai T, Nakamura F, Yoshida K. Increased alpha-taxilin protein expression is associated with the metastatic and invasive potential of renal cell cancer. Biomed Res 2011;32(2):103–10.

[23] Lee MS, Kim RN, H I, Oh DY, Song JY, Noh KW, et al. Identification of a novel partner gene, KIAA1217, fused to RET: functional characterization and inhibitor sensitivity of two isoforms in lung adenocarcinoma. Oncotarget 2016;7(24):36101–14.

[24] Xi R, Pun IH, Menezes SV, Fouani L, Kalinowski DS, Huang ML, et al. Novel thiosemicarbazones inhibit lysine-rich carcinoembryonic antigen-related cell adhesion molecule 1 (CEACAM1) coisolated (LYRIC) and the LYRIC-induced epithelial-mesenchymal transition via upregulation of N-Myc downstream-regulated gene 1 (NDRG1). Mol Pharmacol 2017;91(5):499–517.

[25] Dos Santos M, da Cunha Mercante AM, Nunes FD, Leopoldino AM, de Carvalho MB, Gazito D, et al. Prognostic significance of NDRG1 expression in oral and oropharyngeal squamous cell carcinoma. Mol Biol Rep 2012;39(12):10157–65.

[26] Zheng Y, Xu B, Zhao Y, Gu H, Li C, Wang Y, et al. CA1 contributes to microcalcification and tumourigenesis in breast cancer. BMC Cancer 2015;15:679.

[27] Wang DB, Lu XK, Zhang X, Li ZG, Li CX. Carbonic anhydrase 1 is a promising biomarker for early detection of non-small cell lung cancer. Tumour Biol 2016;37(1):553–9.

[28] Supuran CT. Carbonic Anhydrase inhibition and the management of hypoxic tumors. Metabolites 2017;7(3).

[29] Yang JS, Lin CW, Chuang CY, Su SC, Lin SH, Yang SF. Carbonic anhydrase IX overexpression regulates the migration and progression in oral squamous cell carcinoma. Tumour Biol 2015;36(12):9517–24.

[30] A phase I, multi-center, open-label, study to investigate the safety, tolerability and pharmacokinetic of SLC-0111 in subjects with advanced solid tumours. 2016 [15 January 2018]. Available from: https://clinicaltrials.gov/ct2/show/NCT02215850.

[31] Lundy FT, Orr DF, Gallagher JR, Maxwell P, Shaw C, Napier SS, et al. Identification and overexpression of human neutrophil alpha-defensins (human neutrophil peptides 1, 2 and 3) in squamous cell carcinomas of the human tongue. Oral Oncol 2004;40(2):139–44.

[32] Wang N, Feng Y, Wang Q, Liu S, Xiang L, Sun M, et al. Neutrophils infiltration in the tongue squamous cell carcinoma and its correlation with CEACAM1 expression on tumor cells. PLoS ONE 2014;9(2):e89991.

[33] Bresnick AR, Weber DJ, Zimmer DB. S100 proteins in cancer. Nat Rev Cancer 2015;15(2):96–109.

[34] Dey KK, Bharti R, Dey G, Pal I, Rajesh Y, Chavan S, et al. S100A7 has an oncogenic role in oral squamous cell carcinoma by activating p38/MAPK and RAB2A signaling pathway. Cancer Gene Ther 2016;23(11):382–91.

[35] Tripathi SC, Matta A, Kaur J, Grigull J, Chauhan SS, Thakar A, et al. Nuclear S100A7 is associated with poor prognosis in head and neck cancer. PLoS ONE 2010;5(8):e11939.

[36] 0794GCC: Pentamidine in Treating Patients With Relapsed or Refractory Melanoma [Internet]. Bethesda (MD): National Library of Medicine (US). August 8, 2008 [cited March 30, 2017]. Available from: https://ClinicalTrials.gov/show/NCT00729807.

[37] Clapham DE. Calcium signaling. Cell 2007;131(6):1047–58.

[38] Cui C, Merritt R, Fu L, Pan Z. Targeting calcium signaling in cancer therapy. Acta Pharm Sin B 2017;7(1):3–17.

[39] Hedberg ML, Goh G, Chiosea SI, Bauman JE, Freilino ML, Zeng Y, et al. Genetic landscape of metastatic and recurrent head and neck squamous cell carcinoma. J Clin Invest 2016;126(1):169–80.

[40] Tang D, Tao D, Fang Y, Deng C, Xu Q, Zhou J. TNF-alpha promotes invasion and metastasis via NF-Kappa B pathway in oral squamous cell carcinoma. Med Sci Monit Basic Res 2017;23:141–9.

[41] Peng Q, Deng Z, Pan H, Gu L, Liu O, Tang Z. Mitogen-activated protein kinase signaling pathway in oral cancer. Oncol Lett 2018;15(2):1379–88.

[42] Moll R, Divo M, Langbein L. The human keratins: biology and pathology. Histochem Cell Biol 2008;129(6):705–33.

[43] Barak V, Goike H, Panaretakis KW, Einarsson R. Clinical utility of cytokeratins as tumor markers. Clin Biochem 2004;37(7):529–40.

[44] Mikami Y, Fujii S, Nagata K, Wada H, Hasegawa K, Abe M, et al. GLI-mediated Keratin 17 expression promotes tumor cell growth through the anti-apoptotic function in oral squamous cell carcinomas. J Cancer Res Clin Oncol 2017;143(8):1381–93.

[45] Kitamura R, Toyoshima T, Tanaka H, Kawano S, Kiyosue T, Matsubara R, et al. Association of cytokeratin 17 expression with differentiation in oral squamous cell carcinoma. J Cancer Res Clin Oncol 2012;138(8):1299–310.